Rotor aerodynamics in sheared inflow: An analysis of out-of-plane bending moments

IOP Conf. Series: Journal of Physics: Conf. Series **1037** (2018) 022027 doi:10.1088/1742-6596/1037/2/022027

Rotor aerodynamics in sheared inflow: An analysis of out-of-plane bending moments

Daniel Micallef(1), Tonio Sant(2)

(1)Lecturer, Department of Environmental Design, Faculty for the Built Environment, University of Malta.
(2)Associate Professor, Department of Mechanical Engineering, Faculty of Engineering, University of Malta.

E-mail: daniel.micallef@um.edu.mt

Abstract
A sheared wind profile creates an asymmetric wind field and an asymmetric wind turbine wake. Both of these have been described in the past but a study on their implications on the out-of-plane moment on the rotor is still a gap which needs to be addressed. A numerical assessment has been undertaken using a lifting-line free-wake vortex code. Owing to the lack of experimental validation, two other modelling approaches are used to assess the consistency of results - an actuator disc approach and a blade element momentum approach. Results were found to show acceptably good agreement. The line of action of the thrust force is found to be shifted by around 10% upwards above the rotor axis for the extreme shear case of $\alpha = 0.55$. The wake was found to add to the asymmetry of the wind field by increasing the vertical shift in the line of action by 100% compared to the wind field alone. The results have important implications on the role of the out-of-plane bending moment on the wake kinematics as well as other issues related to fatigue performance of the rotor.

1. Introduction and objectives

Wind turbine rotors operate in a sheared inflow profile over most of their time. The extent of this sheared profile can also be highly variable depending on site conditions. There have been various attempts in the literature to model the resulting rotor aerodynamics and wake using a variety of computational tools ranging from Navier-Stokes solvers using the actuator line technique (see Madsen et al. [2]), actuator disc techniques (see Troldborg et al. [14], free-wake vortex methods (see Madsen et al. [2] and Uzol & Uzol[13]) and even simplified Blade Element momentum approaches by Madsen et al. [2]. Due to the varying inflow with height, the rotor loading is not uniform along the rotor disc, resulting in fluctuating loads with possibly serious implications on fatigue. For a rotor operating in a sheared inflow, the Out-Of-Plane (OOP) bending moment about the horizontal axis of the rotor disc is of particular interest and has seldom been discussed in literature. This moment is dependent on two main components: (i) the variation of the sheared inflow with height and (ii) the asymmetric loading on the rotor disc. Whether or not the wake has a restoring effect in the reduction of the out-of-plane bending moment is the second question which is raised in this work.

In-line with the research questions posed here, the objectives of this work are as follows:

(i) to quantify the upward vertical shift in the line of action of the thrust with respect to the rotor centre;

(ii) To investigate the influence of the wake as either producing a restoring out-of-plane moment or whether it causes a further increase of this moment.

2. Methodology

2.1. The reference rotor

The NREL 5MW rotor is used as the reference rotor (see Jonkman et al. [4]) for this work. An open source lifting line free-wake (FW) vortex model QBlade v0.95 [9] is used as the main approach for this study. Simulations are carried out for the optimal rotor operation with $\lambda = 7$. The rotor hub height is taken as 90m measured from the ground. The wind profile is assumed to follow the power law:

$$V = V_{hub}\left(\frac{y}{H}\right)^{\alpha} \tag{1}$$

where V_{hub} is the velocity at turbine hub height H taken equal to the rated wind speed of 11.4m/s, y is the distance from the ground and α is the shear exponent which determines the extent of the shear. Such a profile is known to be a simplistic representation of the wind profile but the scope of this study is focused on the behaviour of the OOP moment under the influence of a wind shear. Therefore use of a single parameter only, the wind shear exponent is convenient here for simplicity. Furthermore inflow turbulence is assumed to be negligible. It is well known that turbulence influences the wake diffusion and overall behaviour but inclusion of these effects is best studied in future research after the uniform inflow scenario is understood.

2.2. Numerical methods

Due to the lack of experimental data availability for large rotors under shear flow conditions, results from the FW code are cross-compared to those obtained with two other different methods: (i) a Navier-Stokes Actuator Disc (AD) model implemented in the commercial code Fluent v15 [1] and (ii) a Blade Element Momentum (BEM) model using the open source code FASTv8 [5].

All FW simulations are carried out under cases of no shear, $\alpha = 0.1, 0.2$ and 0.55 and with the ground effect switched on or off. The term ground effect here refers to the constraint of no normal flow to the ground. In the FW code this is implemented as a symmetry boundary condition. For the AD model, only the case with ground effect is considered while in the BEM model no consideration to the presence of the ground effect is taken into consideration. For all models, 2D static airfoil data are used.

2.3. Free-Wake code Q-Blade

The Q-Blade code [9] is is used to carry out the FW computations. This code has been used in the past with successful results by Marten et al. [7]. The basic principle behind this code is to discretise the blade into a number of line vortex elements. This also holds for the wake with both trailing and shed vortices corresponding to the radial gradient of the bound circulation and the time derivative of bound circulation respectively. The velocities as a result of all vortex filaments are calculated using the Biot-Savart law:

$$\mathbf{v} = \frac{\Gamma}{4\pi}\int \frac{d\mathbf{l}\times\mathbf{r}}{|\mathbf{r}|^3} \tag{2}$$

In a free wake approach, the wake vortex filament endpoint positions are updated in accordance with the induced velocities at these points. A complete description of the method and algorithm are provided in the Q-blade user manual [9]. Also the method is well documented

in the aerodynamics literature such as Katz and Plotkin [6]. Some important parameters used as input to the model are shown in Table 1 hereunder.

Table 1: Main parameters used for the FW simulation.

Radial elements	50
azimuthal increment	10
number of revolutions	10
Velocity time marching integration	Euler

The simulation results from the free-wake vortex model are verified by considering the periodic convergence of thrust and power in order to ensure that the number of rotor revolutions was enough. Convergence tests on azimuthal and blade radial descritisation were also performed and Table 1 gives the optimal parameters used.

2.4. Actuator disc model

The AD model is based on the that proposed in Troldborg *et al.* [14] and Martinez-Tossas *et al.*[8] and implemented in the commerical code ANSYS Fluent v16.0 [1]. This type of approach has been documented in numerous other sources such as Mikkelsen [12] and Masson *et al.*[10] so here a very general overview is given to maintain the flow of the article. The lift and drag forces are found using the 2D lift and drag coefficient polars for the various airfoil sections found on the NREL 5MW rotor (see Jonkman *et al.* [4]). The lift and drag forces act on individual cells on the actuator disc and hence a solidity factor σ needs to be introduced to apportion the load from an annulus to a sector of the annulus. This is described in more detail in Martinez-Tossas *et al.*[8].

$$L = \sigma \frac{1}{2} \rho V_{rel}^2 c C_L w \tag{3}$$

$$D = \sigma \frac{1}{2} \rho V_{rel}^2 c C_D w \tag{4}$$

where c is the chord, w is the actuator section width, V_{rel} is the relative velocity to the airfoil, C_L is the lift coefficient and C_D is the drag coefficient. The solidity factor is given by:

$$\sigma = \frac{B \Delta A}{A} \tag{5}$$

where B is the number of blades, ΔA is the sector area and A is the rotor swept area πR^2. The axial force component can be found by decomposing the lift and drag forces as follows.

$$F_z = L cos\phi + D sin\phi \tag{6}$$

A linear Gaussian smearing function is used to smear out the rotor loads to ensure stability of the final solution. Critical to this is the regularization parameter $\epsilon = \epsilon_i \Delta z$ as follows:

$$\eta = \frac{1}{\epsilon \sqrt{\pi}} exp \left[\left(-\frac{z}{\epsilon} \right)^2 \right] \tag{7}$$

The variable z is the normal coordinate to the rotor. The value of ϵ_i is taken as 5 in line with the guidelines provided in Martinez-Tossas et al.[8]. The smeared load is the force per unit volume ΔV:

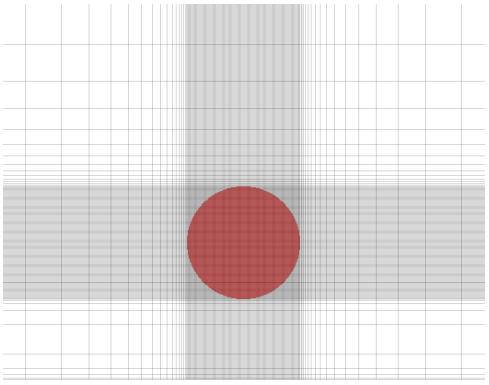

Figure 1: End view of the mesh at the rotor plane and rotor location highlighted in red.

$$f^* = \eta * \frac{F_z}{\Delta V} \tag{8}$$

f^* is implemented as a momentum sink UDF. Convergence tests for mesh independence are carried out using a coarse, medium and fine mesh size. The used mesh resulted in circa 1.5 million cells. The inlet is defined using a User-Defined Function (UDF) profile in accordance with eqn. 1. The opposite end to the inlet is defined as a pressure outlet while the sides and lid of the domain were modelled using a symmetry boundary condition. The ground was modelled as a solid wall. Convergence of residuals and variables are monitored with the former residuals all falling below 10^{-4} and not showing much change with iterations. The velocities are also monitored behind the rotor and no further change with iterations could be observed.

Turbulence is modelled using the SST $k-\omega$ approach of Wilcox [15, 16]. Pressure-velocity coupling was attained using the SIMPLE algorithm while second order upwind discretisation was used for momentum, turbulent kinetic energy and specific dissipation rate. Pressure is also discretised using a second order approach.

2.5. BEM - FASTv8

The BEM computations are carried out with the open source code FAST v8 [5] which was developed by NREL and which implements a modular framework for aero-servo- structural analysis of horizontal-axis wind turbines. The rotor blades and towers are assumed to be rigid by switching off the relevant degrees of freedom. The blade coning and rotor axis tilt angles are set to 0 degrees. The aerodynamic loads are computed using the BEM-based model Aerodyn v15 [5] implemented in FASTv8. A steady wind flow is simulated with the wind shear profile generated using the power law (Eqn. 1). The blades were discretised into 19 elements and only static aerofoil data reported by Jonkman et al. [4] are used. The presence of tower aerodynamic interference was neglected. For each simulation, 600 seconds are modelled with time steps of 0.00625 seconds, allowing sufficient time for the results to stabilise.

3. Results

3.1. Details of the wake asymmetry

The wind field asymmetry causes the wake to similarly behave in an asymmetric manner. This has been documented elsewhere in the literature including Zahle et al.[17], Hansen et al. [3] and Madsen et al. [2]. In order to show this asymmetry in the wake it is worthwhile looking and the vertical components of velocities. Note that the magnitudes of these velocities correspond to the

radial velocities in the blade reference frame but their directions differ. Figure 2 compares these velocities for different shear exponents. The view shown is a side-plane cutting through the wake to visualise the vertical wake asymmetry which is ultimately linked to the OOP moment produced at the rotor disc. The tip and root vortices are clearly visible through this plot. Upstream of the rotor a positive velocity is observed at the top most rotor position since air flows upward around the disc. At the down-most position, the opposite is observed as air flows around this position of the rotor downwards. For the no shear case, the V_z velocity field is rather symmetric about the rotor axis with mostly negative V_z (downward velocity) and positive V_z (upward velocity) at the bottom and top half of the vertical rotor plane. This characteristic of the symmetrical wake expansion. At $\alpha = 0.1$ the bottom half of the vertical plane starts exhibiting a positive V_z at about $\frac{x}{R} = 1.5$. In addition, at the top half of the vertical plane, the positive V_z velocities increase slightly in magnitude when compared to the no shear case. These two phenomena are in fact reflected in the tip vortex paths which travel vertically upwards. When $\alpha = 0.2$, the trends for $\alpha = 0.1$ persist and vertical velocities on the lower half of the vertical side-plane are observed to become positive at around $\frac{x}{R} = 1$ with sharper vertical motion of the tip vortices. The same behaviour is even more accentuated for the extreme shear case of $\alpha = 0.55$ with the vertical upward velocities initiating at around $\frac{x}{R} = 0.5$. The tip vortices on the lower half of the side vertical plane interact with the root vortices at around one rotor diameter. Close to the rotor plane, it is clear that the wake expansion on the down-most rotor position is larger particularly for $\alpha = 0.55$. This effect has been studied and discussed in Madsen et al. [2] attributed to the higher thrust coefficients at this part of the rotor owing to the lower wind velocities at this height. This expansion is counteracted by the vertical velocities created as a result of the tilting or skewing of the helical wake which produces a resulting vertical velocity field. This has also been explained in Sezer-Uzol and Uzol [13] and through analytical vortex ring calculations in Micallef et al. [11].

It is also useful to plot the tip vortex paths in a vertical side plane cutting through the rotor wake. This is shown in Figure 3. These paths are traced from positions of maximum vorticity from the FW calculations. The marked difference in the tip vortex motions occur mostly on the down-most rotor position. The top-most position of the tip vortex paths exhibit a difference in paths at around $\frac{x}{R} = 1.5$. These wake asymmetries are hypothesised to determine the overall OOP at the rotor plane. How this asymmetry combines with the vertical wind field asymmetry is still unclear and will be clarified in the upcoming results.

3.2. Out-of-plane bending moments

Figure 4 shows that the out-of-plane bending moment increases with increasing shear exponent. The Q-Blade and AD results are shown given that both of these include the ground effect. The actuator disc OOP is very close to the mean of the FW results which as is well known varies with azimuth for the shear cases. There is a slight exception to this in the low shear case of $\alpha = 0.1$ where the AD predicts an overall higher OOP.

The case without ground is shown separately in Figure 5 to ensure clarity of figures. In this case the FAST BEM results replace the AD results since the ground effect is not modelled in such a case. The agreement is still on the whole acceptable except for the extreme case of $\alpha = 0.55$ the reason mostly being the non-uniformity in the induction over the rotor azimuth which is not appropriately captured by the BEM type codes. Comparing Figures 4 and 5, the effect of the ground on the OOP can be said to be rather small (around 5% difference) from what is observed with the FW results.

3.3. Thrust force line of action

Figure 6 gives results for the vertical thrust position normalised with rotor radius $\frac{\delta}{R}$ with the ground effect switched on. As with the OOP moment, the line of action of thrust is shifted

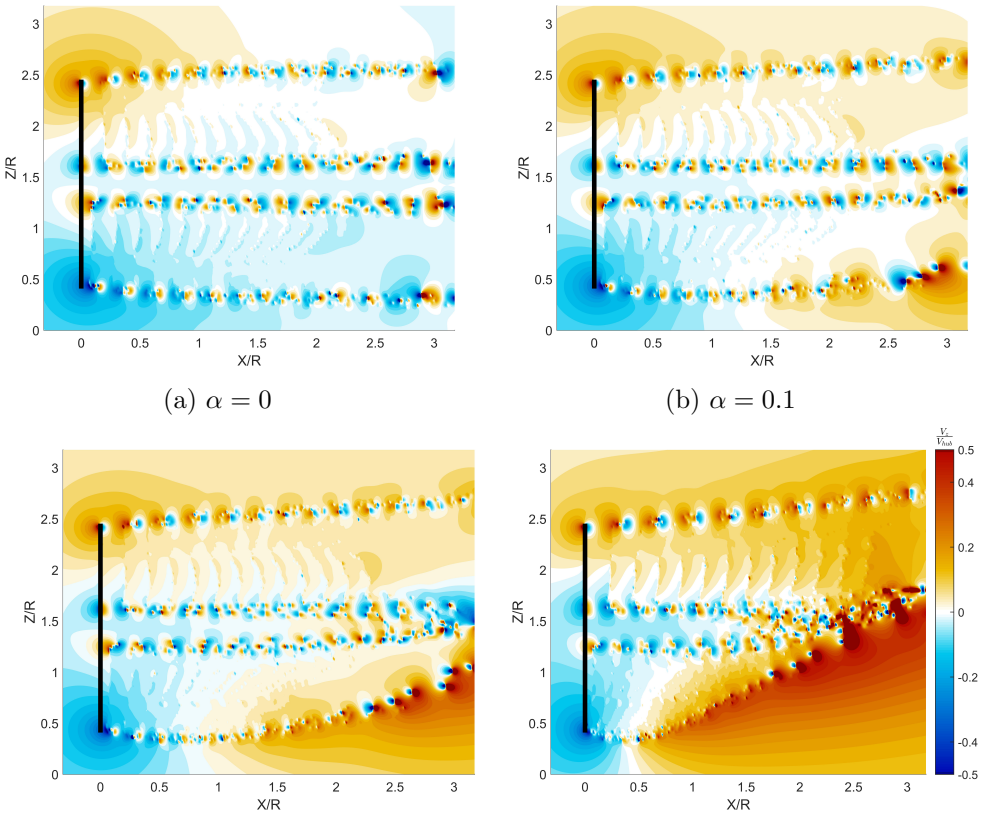

(a) $\alpha = 0$ (b) $\alpha = 0.1$

(c) $\alpha = 0.2$ (d) $\alpha = 0.55$

Figure 2: Velocity in the vertical direction V_z. Velocities shown in a vertical plane for various shear flow exponents. Case shown is when ground effects are turned off.

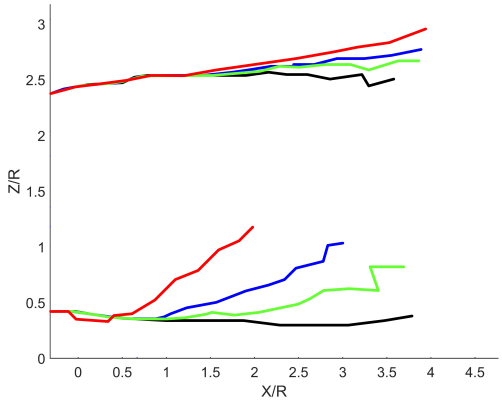

Figure 3: Side view of a vertical plane showing the tip vortex paths. Black: no shear case, Green: $\alpha = 0.1$ case, Blue: $\alpha = 0.2$ and Red: $\alpha = 0.55$.

upwards with increasing shear exponent. Measured from the rotor rotational axis, the line of action of the thrust force does not exceed circa 10% of the rotor radius for even the highest shear of $\alpha = 0.55$. With more moderate shear exponents of 0.2 and 0.1 respectively the thrust force position is below 4% of the rotor radius.

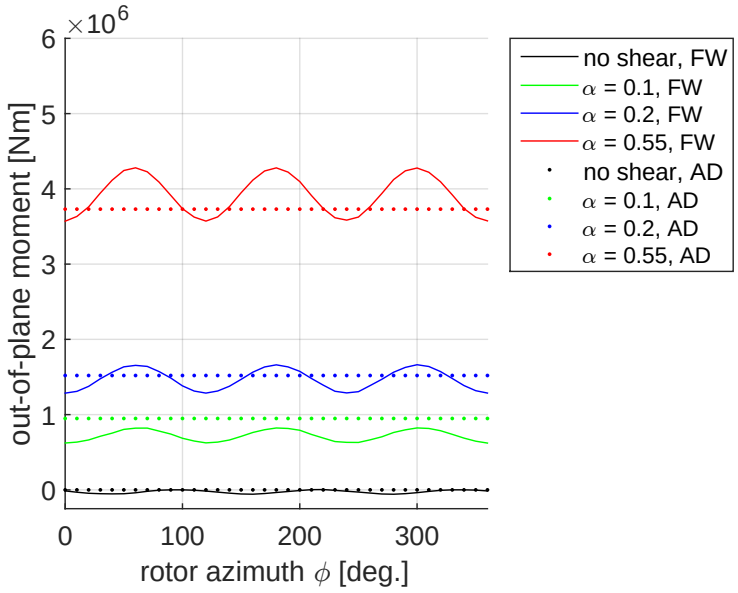

Figure 4: Out-of-plane moment variation (with ground effect) with azimuth for various shear exponents and models used. 'FW' refers to the Q-Blade results and 'AD' refers to the actuator disc results.

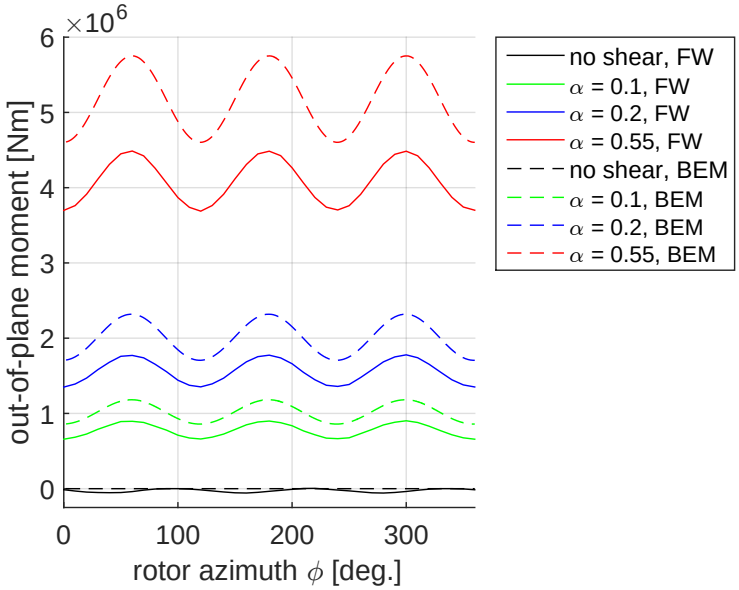

Figure 5: Out-of-plane moment variation (with no ground effect) with azimuth for various shear exponents and models used. 'FW' refers to the Q-Blade results, 'BEM' refers to the FAST results.

The case with 'no ground' is given here for completeness in Figure 7. Only the free wake results change here since for the AD results the ground effect are still on. The difference from the ground effect case are minimal and barely have any effects on the conclusions already made.

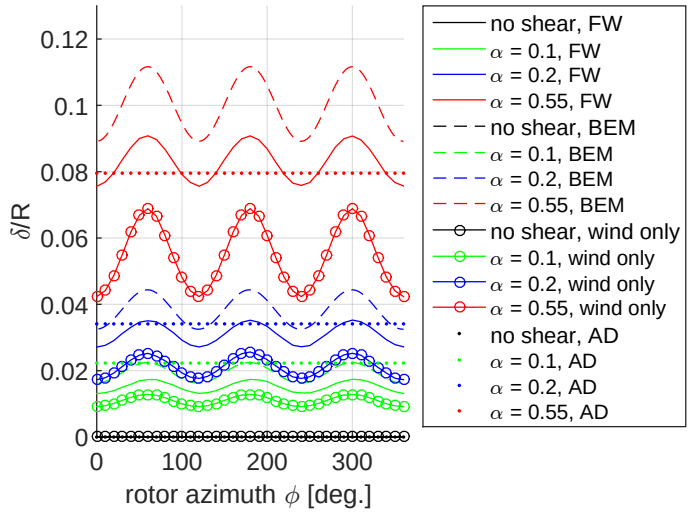

Figure 6: Thrust line of action against blade azimuth with ground effect switched on. 'FW' refers to the Q-Blade results, 'BEM' refers to the FAST results and 'AD' refers to the actuator disc results. 'Wind only' refers to Q-Blade results with the wake vortex filaments switched off.

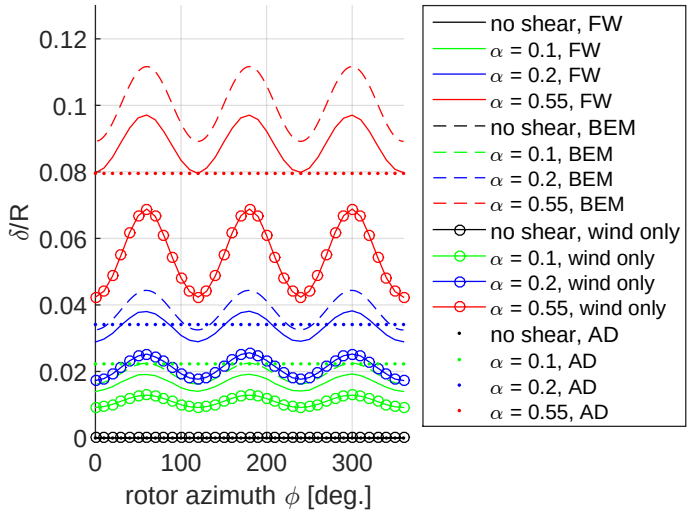

Figure 7: Thrust line of action against blade azimuth with ground effect switched off. 'FW' refers to the Q-Blade results, 'BEM' refers to the FAST results and 'AD' refers to the actuator disc results. 'Wind only' refers to Q-Blade results with the wake vortex filaments switched off.

The plot also shows *Wind only* conditions where the wake vortex elements in the Q-Blade code are switched off. As can be noticed the role of the wake is to shift the line of action of thrust upwards further away from the rotor axis. The extent of this upward shift is a function of the shear exponent with higher wind shears causing larger shifts. This reflects the increasing wake asymmetry caused by higher shear exponents. Considering the FW results, the increase in the vertical shift due to the wake effect is by around 100% when compared to the effects of

the wind only. This is consistent for all shear exponents.

4. Discussion of results

The analysis of wake asymmetry presented earlier is crucial to understand the role of the wake on the OOP moment. Such discussions have been made extensively in the past, particularly during the TORQUE conference of 2010 (see Zahle et al. [17], Hansen et al. [3] and Micallef et al. [11]) where it was debated whether the wake exhibits a gross downward or upward displacement. Subsequent work showed that both do in fact occur at different downstream positions. The work presented here provides insight how these two phenomena influence the OOP moment. The very near wake large expansion and therefore downward wake movement under extreme shear is a phenomenon associated with the differential wind velocities. Contrastingly the gross upward wake motion is associated with an overall balance of angular momentum as a result of the OOP moment. This clockwise moment acting on the rotor can therefore also be thought as causing an equal and opposite moment on the wake which therefore displaces it upwards. In effect, the physical manifestation of this is that the wake helix exhibits a skew and a resulting vertical velocity component which drives it upwards. The extent of this OOP is important in determining the vertical displacement of the wake and hence when investigating rotor to rotor interactions in wind farm environments.

The effect of the 3P variation observed in the results as well as the peak-to-peak variations in the bending moments are important considerations in the fatigue performance of the drive shaft of large scale wind turbine rotors. The asymmetry of the wake has been shown to cause an increase in the OOP bending moment and hence a large shift of the line of action of thrust in the upper portion of the rotor plane. A discussion on this interesting effect is worth putting forward here. If one considers the gross vertical displacement of the wake observed in Figure 3, it is intuitive to suspect that the induction on the upper portion of the rotor increases thus counteracting the higher wind speed due to the wind velocity. From these observations we conclude that this view is not correct and that the very near wake physics, heavily emphasized in the Torque 2010 papers by Zahle et al. [17] and Hansen et al. [3], is clearly more important. The inductions on the upper portion of the rotor become lower given the higher wind velocity and higher on the lower portion of the rotor, resulting in a lower resultant axial velocity. This picture fits the observations of a vertical upward shift of the thrust line of action makes sense. The vertical upward wake shift therefore does not play an important role on the OOP direction even though this cannot be said on the magnitude. Finally it must be mentioned that the OOP of a blade is also influenced by the aero-elastic interaction of the blade with the flow. This may include blade pitching which would certainly have an important implication on the results presented here.

5. Conclusions

The variation of both OOP bending moment and the line of action of thrust on the rotor disc with respect to azimuth has been quantified for various shear exponents in the wind power law using a lifting line potential flow free-wake vortex method implemented in *Q-Blade*. Results have been cross-compared with other numerical procedures including an actuator disc approach (implemented in the commercial code *Fluent*) and the less sophisticated BEM code in *FASTv8*. Experimental data on the NREL 5MW rotor are not available and no direct validation was possible. The main results are summarised hereunder:

(i) Peak-to-peak oscillations in OOP increase with increasing shear exponents

(ii) The role of the wake is to increase the OOP bending moment due to the asymmetrical expansion and evolution

(iii) The vertical wake displacement is for the first time attributed to be due to the reaction moment of the rotor on the wake

(iv) The vertical line of action of thrust does not exceed more than 10% of the rotor radius in the upward portion of the rotor for the most extreme shear exponent considered of $\alpha = 0.55$

(v) The effects of the wake on the vertical shift of the thrust line of action is around 100% more than the effect of the vertical wind profile. This wake effect is mainly associated with the wake physics close to the rotor and the vertical wake shift does not seem to have restoring effect of the OOP as would be expected intuitively.

(vi) Ground effects did not play a major role in any of the above conclusions

The results presented here are based on different wind profiles described by simplistic power law profiles which are known to not represent the wind profile precisely. Nonetheless, the wind profile used using a single variable α as descriptor of the extent of shear is convenient in this case to investigate the effect of the extent of shear on the final results. Some of the conclusions particularly the quantification of the thrust line of action are expected to change depending on the exact wind profile used but nonetheless the overall trends are not expected to be largely different.

Experimental observations are crucially required despite the known difficulty in performing full, large scale wake measurements. The importance of such measurements has been clearly shown here vis-a-vis the vertical wake displacement.

6. References

[1] I. Ansys. ANSYS Fluent Theory Guide. 15317(November):514, 2013.

[2] E. P. H. Aa.Madsen, V. Riziotis, F.Zahle, M.O.L.Hansen, H. Snel, F. Grasso, T. J. Larsen1 and F. Rasmussen. Blade element momentum modeling of inflow with shear in comparison with advanced model results H. *Wind Energy*, 17(April 2013):657–669, 2014.

[3] M. O. L. Hansen, R. F. Mikkelsen, and S. Øye. *Investigating the effect of extreme shear and yaw using an Actuator Line model*, pages 311–316. 2010.

[4] J. Jonkman, S. Butterfield, W. Musial, and G. Scott. Definition of a 5-MW reference wind turbine for offshore system development. *Contract*, (February):1–75, 2009.

[5] J. M. Jonkman and M. L. Buhl Jr. FAST User's Guide. Golden, CO (USA): NREL, 2005.

[6] J. Katz and A. Plotkin. *Low-Speed Aerodynamics*. Cambridge University Press, second edition, 2001.

[7] M. Lennie, C. N. Nayeri, and C. O. Paschereit. GT2015-43265. pages 1–11, 2015.

[8] M. J. C. Luis A. Martínez-Tossas and S. Leonardi. Large eddy simulations of the flow past wind turbines: actuator line and disk modeling. *Wind Energy*, 17(April 2013):657–669, 2014.

[9] D. Marten. QBlade v0.95 Guidelines for Lifting Line Free Vortex Wake Simulations. Technical Report June, 2016.

[10] C. Masson, A. Smaïli, and C. Leclerc. Aerodynamic analysis of HAWTs operating in unsteady conditions. *Wind Energy*, 4(1):1–22, 2001.

[11] D. Micallef, C. J. Simão Ferreira, T. Sant, and G. J. W. van Bussel. An Analytical Model of Wake Deflection Due to Shear Flow. *The Science of making Torque from Wind*, 2010.

[12] R. Mikkelsen, J. N. Sørensen, S. Øye, and N. Troldborg. Analysis of Power Enhancement for a Row of Wind Turbines Using the Actuator Line Technique. *Journal of Physics: Conference Series*, 75:012044, 2007.

[13] Nilay Sezer-Uzol and Oguz Uzol. Effect of steady and transient wind shear on the wake structure and performance of a horizontal axis wind turbine rotor. *Wind Energy*, 17(April 2013):657–669, 2014.

[14] N. Troldborg, M. Gaunaa, and R. Mikkelsen. Actuator disc simulations of influence of wind shear on power production of wind turbines. *Torque 2010, The science of making torque from wind, EWEA*, pages p271–297, 2010.

[15] D. C. Wilcox. Reassessment of the scale-determining equation for advanced turbulence models. *AIAA Journal*, 26(11):1299–1310, 1988.

[16] D. C. Wilcox. *50191605-Turbulence-Modelling-CFD-Wilcox.pdf*. DCW Industries, Inc., California, 2nd edition, 1994.

[17] F. Zahle and N. N. Sørensen. *Upwind Navier-Stokes Rotor Flow Simulations with ground proximity and shear*, pages 255–263. European Wind Energy Association (EWEA), 2010.